

COLLIMATION CLEANING AT THE LHC WITH ADVANCED SECONDARY COLLIMATOR MATERIALS*

E. Quaranta[†], R. Bruce, A. Mereghetti, S. Redaelli, A. Rossi
CERN, Geneva, Switzerland

Abstract

The LHC collimation system must ensure efficient beam halo cleaning in all machine conditions. The first run in 2010-2013 showed that the LHC performance may be limited by collimator material-related concerns, such as the contribution from the present carbon-based secondary collimators to the machine impedance and, consequently, to the beam instability. Novel materials based on composites are currently under development for the next generation of LHC collimators to address these limitations. Particle tracking simulations of collimation efficiency were performed using the Sixtrack code and a material database updated to model these composites. In this paper, the simulation results will be presented with the aim of studying the effect of the advanced collimators on the LHC beam cleaning.

INTRODUCTION

The collimation system of the CERN Large Hadron Collider (LHC) is designed to efficiently absorb high energy beam losses and assure machine protection [1, 2]. Its multi-stage architecture is based on primary and secondary collimators (TCPs and TCSGs, respectively), made of a carbon-fiber-carbon composite (CFC). This choice has been made to guarantee good thermal stability and high robustness against beam induced losses for the collimators with the jaws the closest to the beam. Tungsten-based tertiary collimators (TCTs) and absorbers with higher particle stopping potential are instead devoted to protect the LHC experimental regions and reduce the background to experiments, at the expense of robustness against beam losses.

Since the first design of the present system [2], non-metallic collimators largely contribute to the impedance of the whole machine [3], mainly because of the low electrical conductivity of the CFC. The impedance is an electromagnetic concern of paramount importance in particular for the High Luminosity (HL) upgrade of the LHC [4], which aims at doubling the bunch intensity and at reducing the beam emittance.

Consequently, an intense R&D program has started at CERN to explore novel materials for new collimator jaws which could possibly replace some of the present CFC ones. The idea is to combine the excellent thermal properties of graphite or diamond with those of metals and metal-based ceramics of high mechanical strength and, above all, good electrical conductivity. The most promising materials iden-

tified so far are Molybdenum Carbide - Graphite (MoGr) composite and Copper-Diamond (CuCD) composite [5].

The effect of novel composite materials on the cleaning performance of the LHC collimation system must be investigated and the results used to complete the picture of the collimator material specifications. Therefore, a palette of materials is implemented in the tools used for LHC halo cleaning simulations. The first outcomes of the study are presented in this paper.

IMPLEMENTATION OF NEW MATERIALS IN SIXTRACK

The particle tracking code Sixtrack with collimation features [6–8] was upgraded to implement new composite materials. This setup is used as state-of-the-art simulation tool for collimation studies at the LHC. When energetic particles interact with matter, as for the LHC proton beams with the collimator material, scattering mechanisms occur. These mechanisms are reproduced in SixTrack by a Monte-Carlo code deriving from the K2 scattering routine [9], which has been also recently reviewed and improved [10].

Four composite materials, some of them already used in present collimators and others of interest for future collimation upgrades, have been added to the existing material database in SixTrack: MoGr and CuCD as alternatives to CFC for primary and secondary collimators; Inermet180, a tungsten heavy alloy used in the jaws of tertiary collimators and absorbers; Glidcop, a copper-based composite.

The routine treats mono-element materials. Thus, composite materials are dealt with by calculating off-line “effective” input parameters starting from material composition, as discussed below. The most important ones are listed in Table 1, along with the composition. For comparison, the same table lists CFC, already coded in SixTrack as pure carbon.

The atomic number Z and atomic weight A of each compound material was derived as average weighted on the atomic fraction of their components

$$p = \sum_i at_i \cdot p_i, \quad (1)$$

where p is the property of the compound to be computed, p_i are the values of the property, extracted from the Particle Data Group database [11], for the i -th element present in the material and at_i the atomic content of each element in the composite.

While traversing a medium and interacting with the electromagnetic field of the target atoms, a charged particle may lose energy by ionization according to the Bethe-Bloch

* Research supported by EU FP7 HiLumi LHC (Grant agree. 284404) and EuCARD-2 (Grant agree. 312453)

[†] elena.quaranta@cern.ch

Table 1: Summary of the Properties of the New Composite Materials Added in SixTrack: average atomic number Z , average atomic weight A , density ρ , electrical conductivity σ_{el} , composition by atomic fractions, radiation length χ_0 , collision length λ_{tot} and inelastic scattering length λ_{inel} for 200 GeV/c protons. The values for CFC, already implemented in the code, are reported for reference.

	Z	A [g/mol]	ρ [g/cm ³]	σ_{el} [MS/m]	at. content [%]	χ_0 [cm]	λ_{tot} [cm]	λ_{inel} [cm]
CFC	6	12.01	1.67	0.14	100 C	25.57	35.45	51.38
MoGR	6.653	13.532	2.5	1	2.7 Mo ₂ C, 97.3 C	11.931	24.84	36.42
CuCD	11.898	25.238	5.4	12.6	25.7 Cu, 73.3 CD, 1 B	3.162	13.56	20.97
Glidcop	28.823	63.149	8.93	53.8	99.1 Cu, 0.9 Al ₂ O ₃	1.442	9.42	15.36
Inermet180	67.657	166.68	18	8.6	86.1 W, 9.9 Ni, 4 Cu	0.385	6.03	10.44

formula [12] and may undergo several deflections of its trajectory due to elastic collisions with the medium nuclei (Multiple Coulomb Scattering). The mean ionization energy I and the radiation length χ_0 must be provided to SixTrack to correctly simulate these events. For a composite materials, these values can be approximated by [11]

$$\frac{1}{p} = \sum_i \frac{wt_i}{Pi}, \quad (2)$$

where wt_i is the mass fraction of the i -th element in the compound. Once more, p_i refer to values in [11].

At some point, the incoming protons will interact with the nuclei of the material in different ways. Each process is characterized by its cross section (σ), that gives the probability for the scattering process to occur in a specific material. The total nuclear cross section (σ_{tot}) takes into account elastic, inelastic and single diffractive events [13]. The total and inelastic cross sections (σ_{inel}) at 450 GeV were implemented in SixTrack, calculated as follows

$$\sigma = \frac{A}{N_A \rho \lambda}, \quad (3)$$

with N_A Avogadro's number, A and ρ the average atomic weight and the density of the material, respectively. For composite materials, the collision length (λ_{tot}) and the inelastic length (λ_{inel}) are calculated as in Eq. (2).

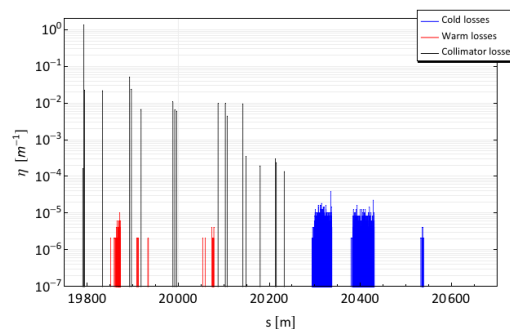
CLEANING SIMULATIONS WITH ADVANCED COLLIMATOR MATERIALS

Table 2: Collimator Settings Used for the SixTrack Simulation. The values are expressed in units of standard deviation of the beam, calculated for a normalized emittance of 3.5 μm rad.

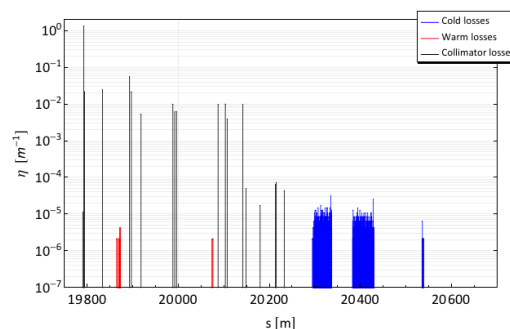
Collimator Families	Settings [σ]
IR7 TCP / TCSG / TCLA	6 / 7 / 10
IR3 TCP / TCSG / TCLA	15 / 18 / 20
IR6 TCSG / TCDQ	7.5 / 8
IR1/5 TCTs	8.3
IR2/8 TCTs	25

In order to study the effect of the new collimator materials on the collimation cleaning efficiency, SixTrack simulations

were performed with the full LHC collimation system in place. The horizontal halo case was studied for the nominal 7TeV machine, with optics squeezed to 55cm. Collimator settings are listed in Table 2. Three different cases were simulated where all the secondary collimator jaws in the betatron cleaning insertion (IR7) were either made of MoGR, CuCD or Inermet180 instead than the present CFC. The high-Z option of Inermet180 is actually not in any upgrade plan because of its limited robustness but it was included in this study for comparison purposes.



(a) CFC secondary collimators in IR7



(b) CuCD secondary collimators in IR7

Figure 1: Distribution of losses in IR7 for two simulated cases.

As shown in Fig. 1, losses in the cold dispersion suppressor magnets around IR7, which represent the location of highest losses for the present system, are not affected in a significant way by the material choice of secondary collimators. This result is expected because these losses are dominated by single diffractive interactions taking place in the TCPs [14] that are unchanged in these studies.

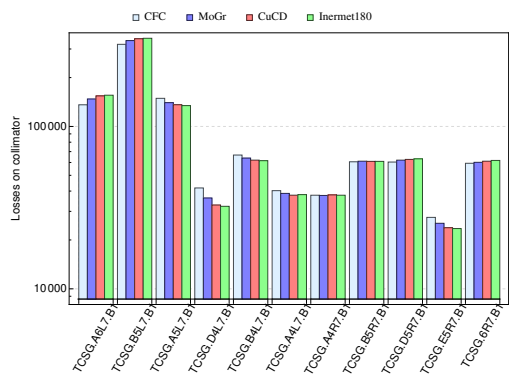


Figure 2: Simulated losses on secondary collimators in IR7 for different jaw materials.

We instead focus the analysis on the loss distributions along the IR7 collimators, in particular at the TCSGs, by looking at the distributions of inelastic interactions in the jaw volume. This is given for all TCSGs in Fig. 2 and for 4 simulation cases (CFC is included as a reference). It is shown that the first two secondary collimators downstream of the primary collimators are progressively more loaded as the effective Z of the composites increases. These are the secondary collimators that intercept the products of the scattering with the primary collimators and larger Z values have a direct impact on the absorption of particles. Differences in losses in the TCSGs further downstream are less apparent and, if any, indicate lower loads for the new materials than for the present CFC. This is mainly caused by the fact that a larger fraction of secondary halo is absorbed by the first two secondaries.

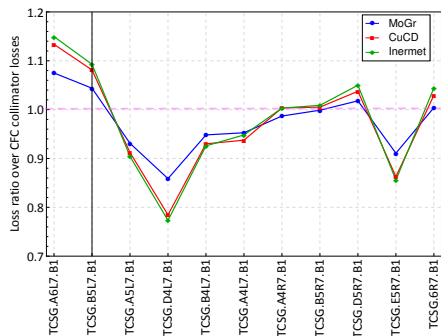


Figure 3: Ratio between simulated losses on secondary collimators in IR7 for different jaw materials over the CFC ones.

The loss ratio calculated collimator by collimator for each new material over the standard CFC (Fig. 3) shows an increase by 15% in the worst case. Accounting for an additional factor 2 for HL-LHC beam intensity, the load on collimators due to beam impact appears still compatible with the present estimates of dynamic deformation limits during beam losses [15]. If confirmed by energy deposition studies, this preliminary conclusion would be a first important outcome of this study, indicating that the present collimator design remain mechanically adequate if only materials

inserts are changed, without major upgraded of the cooling and positioning control systems.

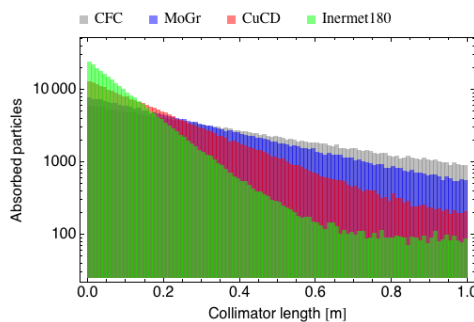


Figure 4: Distribution of particles lost along the length of the most loaded TCSG in IR7.

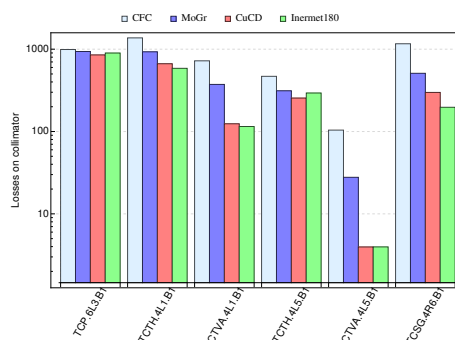


Figure 5: Losses on collimators in other IPs when different materials in IR7 secondary collimators are simulated.

The distribution of the particles absorbed along the length of both jaws in the most loaded secondary collimator (TCSG.B5L7.B1), Fig. 4, shows an exponential decrease due to inelastic scattering events, steeper for materials with higher density and atomic number, as expected. The flatter behaviour visible in the case of Inermet180 beyond 60 cm is due to particles hitting the jaw not on the front face but on the side. For the other materials, this is hidden by the exponential trend.

Moreover, collimators in other locations in the LHC would benefit from the replacement of CFC secondary collimators in IR7: as shown in Fig. 5, the load is significantly reduced when advanced material collimators are used.

CONCLUSIONS

Compound materials have been successfully implemented in SixTrack and are available for simulations of collimation cleaning at the LHC. This implementation relies on the calculation of effective material properties such as cross sections and radiation lengths. We presented first simulation results of halo cleaning in the LHC ring using novel materials for the secondary collimators instead of CFC. This preliminary study will be followed by a detailed comparison with other tools for simulating the interactions of proton beams with matter, before proceeding with a more extensive simulation campaign to address relevant scenarios of LHC upgrades.

REFERENCES

- [1] LHC design report v.1. *CERN-2004-003-V1*.
- [2] R.W. Assmann *et al.* TUODFI01. *EPAC06*.
- [3] N. Mounet *et al.* Collimator impedance measurements in the LHC. *IPAC13, Shanghai, China*, 2013.
- [4] L. Rossi *et al.* High Luminosity Large Hadron Collider. A description for the European strategy preparatory group. *CERN-ATS-2012-236*, 2012.
- [5] A. Bertarelli *et al.* Novel materials for collimators at LHC and its upgrades. *HB2014, East Lansing, Michigan*, 2014.
- [6] F. Schmidt. *CERN/SL/94-56-AP*.
- [7] <http://sixtrack-ng.web.cern.ch/sixtrack-ng/>.
- [8] G. Robert-Demolaize. PhD thesis, Grenoble, 2006.
- [9] <http://lhc-collimation-project.web.cern.ch/lhc-collimation-project/code-tracking.htm>.
- [10] C. Tambasco. Master thesis. roma. 2014.
- [11] K.A. Olive *et al.* Particle Data Group. *Chin. Phys. C*, 38, 090001, 2014.
- [12] K. Nakamura *et al.* Passage of particles through matter. *JPG* 37, 075021, 2010.
- [13] N. Catalan Lasheras. PhD thesis, Zaragoza, 1998.
- [14] C. Bracco. PhD thesis, EPFL Lausanne, 2008.
- [15] A. Bertarelli *et al.* Updated robustness limits for collimator material. *LHC Machine Protection Workshop, Annecy, France*, 2013.